Prevalence of exponential bed thickness distributions in the stratigraphic record: Experiments and theory

Kyle M. Straub,[1] Vamsi Ganti,[2] Chris Paola,[3] and Efi Foufoula-Georgiou[2]

[1] Stratigraphy preserved in alluvial basins holds important information for reconstructing past environmental conditions via inversion methodologies. In this paper we explore, through the use of physical and numerical experiments, the forward problem, that is, we quantify how the probabilistic structure of the processes that govern the evolution of depositional systems relates to the probability distribution of the preserved bed thicknesses. We demonstrate that the extreme variability, as evidenced by heavy-tailed distribution of the surface elevation increments, largely cancels itself out in the resulting stratigraphy. Specifically, we show that bed thickness is well described by an exponential distribution even when erosional and depositional increments characterizing the surface evolution exhibit heavy-tailed statistics, i.e., large, infrequent events have a significant chance of occurrence. We attribute this finding to the symmetric nature of the distribution of elevation increments (both erosional and depositional events) and the additive nature of the stratigraphic filter. We also show that the variability of surface elevation increments, as measured by the interquartile range of their probability distribution, has a robust and well-defined relationship with the preserved mean bed thickness.

1. Introduction

[2] The accumulation of sediment, even in strongly net depositional environments, is an unsteady process [*Ager*, 1993] and in most environments, sedimentation and erosion rates vary over a wide range of temporal and spatial scales [*Gardner et al.*, 1987; *Paola*, 2000; *Sadler*, 1981]. Changes in sedimentation/erosion rates, and in particular transitions between erosion and deposition, are often associated with lateral and vertical changes in the texture of sedimentary deposits. This texture in turn results from spatial changes in grain size of deposited particles and typically marks stratal boundaries. In one (vertical) dimension, the intervals between these boundaries define bed thickness, i.e., the thicknesses of individual strata. In the common case where change between erosion and deposition is associated with migrating topography, one would expect some relation between the statistical properties of the topography and those of the preserved beds. The purpose of this paper is to investigate this relationship.

[3] Over the past thirty years studies related to the generation of stratigraphy in one dimension have primarily focused on quantifying the "completeness of time" preserved in the stratigraphic record. This line of research initiated with a paper by *Sadler* [1981] who found that the deposition rate decreases as a power law function of the interval of time over which deposition rate is measured. This simple yet powerful observation motivated several studies on the statistical structure of surface elevation increments as they pertain to the construction of 1D stratigraphic columns [*Jerolmack and Sadler*, 2007; *Pelletier and Turcotte*, 1997; *Schumer and Jerolmack*, 2009; *Strauss and Sadler*, 1989; *Tipper*, 1983], mainly using 1D stochastic diffusion models of sedimentation. While these studies produced significant advances in our understanding of how time is recorded within stratigraphy, questions about the distribution of preserved bed thickness remain: what dictates the distribution of bed thicknesses preserved in stratigraphy and how do measurements of bed thickness (simple to obtain in comparison to measurements of deposit age) relate to the nature of the surfaces that created them?

[4] Several recent studies suggest that the shape, extent, and distribution of stratal boundaries are not merely functions of instantaneous paleo-topography, but can be quantified as functions of three characteristics of the geomorphological system: 1) the statistics describing the time-variant topography of an actively changing surface, 2) the kinematics by which the surface is changing, and 3) the rate of net deposition [*Martin*, 2007; *Paola et al.*, 2009; *Strong and Paola*, 2008]. While this formulation for quantifying the architecture of stratigraphy is becoming increasingly accepted, we still lack predictive methods to reconstruct surface

[1]Department of Earth and Environmental Sciences, Tulane University, New Orleans, Louisiana, USA.
[2]St. Anthony Falls Laboratory, Department of Civil Engineering, University of Minnesota, Minneapolis, Minnesota, USA.
[3]St. Anthony Falls Laboratory, Department of Geology and Geophysics, University of Minnesota, Minneapolis, Minnesota, USA.
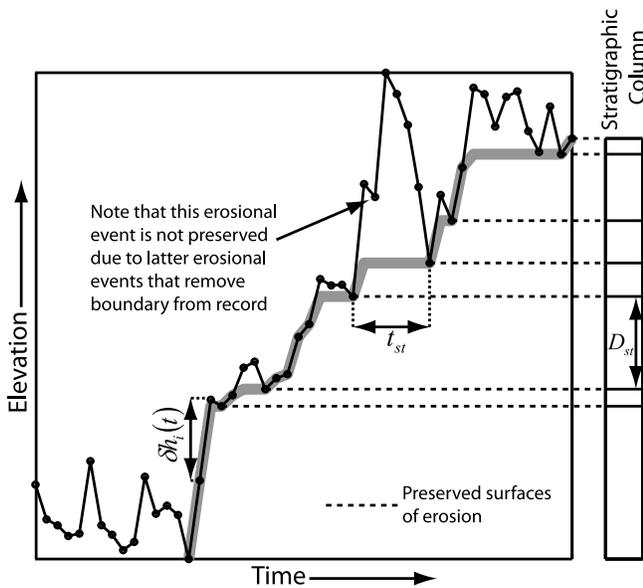
Figure 1. Schematic diagram illustrating the construction of a stratigraphic column from elevation increments. Preserved stratigraphic beds occur in environments where the long-term mean of the elevation increments, $\delta h_i(t)$, is positive. Beds in this study are defined as depositional bodies bounded above and below by preserved erosional surfaces.

topography from preserved stratigraphy, with only a few notable exceptions [*Endo*, 2010; *Jerolmack and Mohrig*, 2005; *Leclair and Bridge*, 2001]. The construction of such inverse predictive methods has the potential to unlock paleo-surface history stored in the stratigraphic record.

[5] The seminal work by *Kolmogorov* [1951] on the relationship between preserved bed thicknesses and the distributions of the erosional and depositional events that form them remains one of the most complete quantitative theories in stratigraphy. In this work, Kolmogorov presented an analytical derivation of the distribution of bed thicknesses and showed that it is a truncated distribution whose shape relates to the distribution of depositional and erosional events in a given setting. In the Kolmogorov model, the construction of stratigraphy is attributed to the summation of depositional and erosional events. A stratigraphic section can be subdivided into a series of beds, where a bed is described as a package of sediment bounded above and below by surfaces of erosion (Figure 1). This stochastic sequence of depositional ($\delta h_e > 0$) and erosional events ($\delta h_e < 0$) produces a set of beds with varying degrees of stratigraphic completeness. The frequency distribution of the depositional and erosional events, $f(\delta h_e)$, which was assumed to be Gaussian in shape by *Kolmogorov* [1951], spans over a range of positive and negative values with occasional extreme events on either side. As erosion removes material from the stratigraphic record, the distribution of the preserved sequence of beds, D_{st}, is truncated at zero leaving only positive values (Figure 2). Kolmogorov showed that the probability density of preserved bed thickness, $f(D_{st})$, can be related to the distribution of depositional and erosional events, $f(\delta h_e)$, by $f(D_{st}) = f(\delta h_e)/K_c$, where K_c is termed the Kolmogorov coefficient that takes a value between 0 and 1. The dimensionless Kolmogorov coefficient represents the long-term

fraction of depositional events preserved in a given alluvial basin. Following this work, *Dacey* [1979] proposed a derivation relating the thickness of beds to incremental elevation changes. In this work, Dacey provided a derivation for an exponential distribution of bed thicknesses from exponentially distributed depositional and erosional increments.

[6] As elegant as *Kolmogorov*'s [1951] theory is, it is based on the statistics of erosional and depositional events, not on the statistics of topography itself. Hence *Paola and Borgman* [1991] proposed a method that directly linked preserved bed thickness to topography. Their method yielded an analytical relation between the variance of topography and the probability density function (PDF) of bed thickness, but only in the case when net rate of deposition was zero, and only for exponential-type topographic PDFs. Our specific goal in this paper is to extend this line of work to the full range of topographic PDFs and rates of net deposition, as a step toward advancing our quantitative ability of inverting bed thickness statistics for information about paleotopography.

[7] While only a few studies examine quantitatively the link between surface elevation increments and bed thickness statistics, several field studies have examined the statistical distribution of preserved bed thickness. For example, *Rothman et al.* [1994] presented measurements of turbidite bed thicknesses and reported that these are well described by a power law distribution, while data presented by *Talling* [2001] and *Sylvester* [2007] were best fit by lognormal distributions. Critical to the discussion of bed thickness distributions is the definition of a bed itself. Spatial changes in the texture of sedimentary sections can result from a range of processes. For example, in environments with frequent alternation between erosion and deposition, textural horizons bounding deposits are often associated with unconformities (i.e., erosional boundaries) and the boundaries result from alternation of erosion and deposition. We term
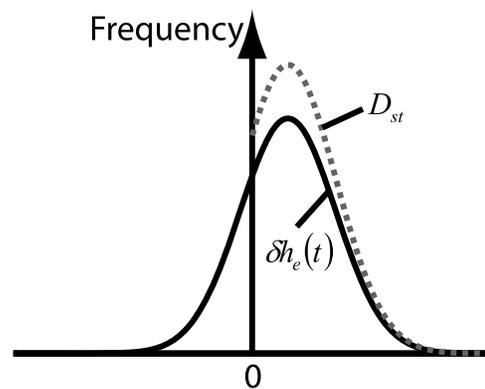

Figure 2. Kolmogorov's model of truncated bed thickness distributions. In Kolmogorov's model the frequency distribution, $f(\delta h_e)$, of both depositional and erosional events spans a negative (erosion) to positive (deposition) range. Because erosion removes material from the stratigraphic record, the resulting distribution of bed thicknesses spans only positive values and is thus a left-side truncated frequency distribution, $f(D_{st})$ of bed thicknesses, and has a form that is related through the Kolmogorov coefficient to the positive-value side of $f(\delta h_e)$.

these beds "unconformity-bounded beds." In comparison, textural horizons bounding deposits of purely depositional flows are also possible; for example, in purely depositional turbidity currents, beds are primarily associated with the stacking of coarse sediment from deposition by the body of one flow on top of fine grain sediment deposited by the tail of a preceding turbidity current [e.g., *Bailey and Smith*, 2010; *Carlson and Grotzinger*, 2001; *Pirmez et al.*, 1997; *Rothman et al.*, 1994; *Sinclair and Cowie*, 2003]. The differences between the two bed definitions above have implications for how one inverts bed thickness distributions for paleo-surface dynamics. The latter case, for convenience termed a "paraconformity-bounded bed," bed thicknesses can easily be mapped to the elevation increments that formed them as the full time sequence of elevations is preserved in the depositional record. The PDF of bed thickness in the paraconformity-bounded case cannot differ from the PDF of elevation fluctuations, so for instance a power law distribution of purely depositional turbidite bed thicknesses implies a power law distribution of the size/duration of individual turbidity current events. Other settings prone to the production of paraconformity-bounded beds include regions with rapid lithification and high resistance to erosion, such as peritidal carbonate settings [*Drummond and Dugan*, 1999]. The relationship between unconformity bounded beds and the elevation fluctuations that formed them is more difficult to assess due to the removal of sediment during incision. Several studies that define beds as deposits bounded by erosional surfaces report exponential distributions for bed thicknesses in a range of environmental settings and for a range of spatial scales [*Beeden*, 1983; *Drummond and Wilkinson*, 1996; *Mizutani and Hattori*, 1972; *Muto*, 1995]. In the remainder of this paper we will explore only the unconformity-bounded beds and their relationship to surface elevation increments.

[8] While bed thickness measurements from stratigraphic records are ample and can be used to characterize their probability distribution, measurements of the elevation increments or surface morphodynamics that created those bed thicknesses are rare at best. This is in part due to the difficulty of obtaining time series of elevations long enough to characterize large-magnitude, low-frequency events (e.g., avulsions). As such, we lack enough data from natural systems to determine even the general family (e.g., exponential, power law, etc.) of distributions that best describe elevation increments in alluvial basins and other environments. It is noted that the *Kolmogorov* [1951] model uses a Gaussian distribution while the work of *Dacey* [1979] uses an exponential distribution for elevation increments to derive the distribution of the preserved bed thickness. However, several recent sediment transport studies have reported heavy-tailed distributions for sediment transport and elevation fluctuations both in river morphodynamics and in hillslope and coupled river-hillslope systems [*Foufoula-Georgiou et al.*, 2010; *Ganti et al.*, 2010; *Stark et al.*, 2009]. In this paper we use data from a physical experiment on a fluvial system in an experimental basin experiencing relative subsidence to characterize the statistics associated with the fluvial dynamics occurring over a range of time-scales and relate these surface statistics to the resulting bed thickness distributions. During this experiment, elevation was monitored at a temporal frequency comparable to the time-scale

of the system's "meso-scale dynamics" [*Paola*, 2000; *Sheets et al.*, 2002] and over a duration long enough to generate reliable statistics on the magnitude of elevation increments. In a recent paper, *Ganti et al.* [2011] used data from this experiment to quantify, for the first time, heavy-tailed statistics in the surface dynamics of aggrading deltas. That study raised the question as to why so many observations from field scale stratigraphy show exponential PDFs for bed thickness despite the possible heavy-tailed statistics of surface topography. In this paper we further probe into this question and demonstrate via analysis of the experimental data and extensive numerical simulations the reasons and conditions under which extreme fluctuations in bed elevation series (e.g., abrupt and large erosional and depositional events) do not get recorded in the stratigraphic record. We also provide a relationship between the preserved mean bed thickness and the variability of the bed elevation increments and show that this relationship remains robust under different probabilistic structures of the alluvial surface dynamics. We propose the interquartile range (defined as the difference between the 75th and 25th quartile of the bed elevation fluctuations) as the proper measure of variability since the heavy-tailed power law distribution of elevation increments suggests theoretical distributions for which the standard variance (second moment around the mean) might not always be properly defined.

2. Experimental Methods

2.1. Description of the Experiment

[9] The experiment discussed here (DB-03) was performed and originally documented by *Sheets et al.* [2007]. The main focus of the work of *Sheets et al.* [2007] was documenting the creation and preservation of channel-form sand bodies in alluvial systems. Since this initial publication, data from the DB-03 experiment have been used in studies on compensational stacking of sedimentary deposits [*Straub et al.*, 2009] and clustering of sand bodies in fluvial stratigraphy [*Hajek et al.*, 2010]. In this section we provide a short description of the experimental setup. For a more detailed description see *Sheets et al.* [2007].

[10] The motivation for the DB-03 experiment was to obtain detailed records of fluvial processes, topographic evolution and stratigraphy, with sufficient spatial and temporal resolution to observe and quantify the formation of channel sand bodies. The experiment was performed in the Delta Basin at St. Anthony Falls Laboratory at the University of Minnesota. This basin is 5 m by 5 m and 0.61 m deep (Figure 3). Accommodation is created in the Delta Basin by slowly increasing base level by way of a siphon-based ocean controller. This system allows for the control of base level with mm-scale precision [*Sheets et al.*, 2007].

[11] The experiment included an initial buildout phase in which sediment and water were mixed in a funnel and fed into one corner of the basin while base-level remained constant. The delta was allowed to prograde into the basin and produced an approximately radially symmetrical fluvial system. After the system prograded 2.5 m from source to shoreline a base-level rise was initiated. Subsidence in the Delta Basin was simulated via a gradual rise in base level, at a rate equal to the total sediment discharge divided by the desired fluvial system area. This sediment feed rate allowed
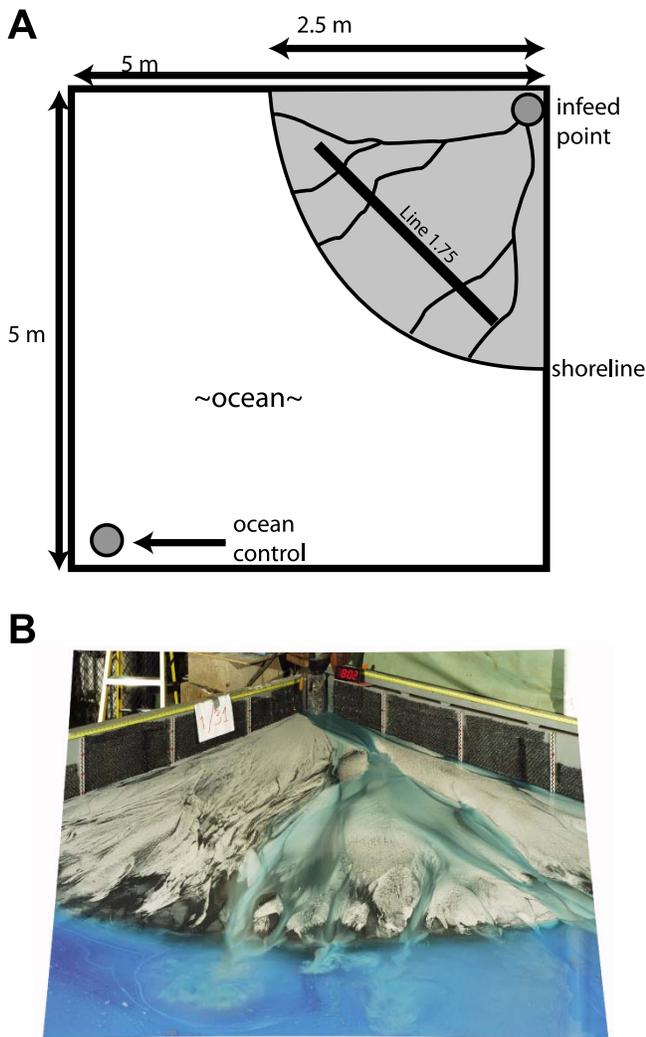
A

B

Figure 3. Schematic diagram and photograph of the Delta Basin facility and DB-03 experiment. (a) Position of the topographic transects is indicated by a solid black line on the fluvial surface. Note that the base-level control drain is in the opposite corner of the basin from the infeed point. (b) Photograph taken approximately 15.0 h in the DB-03 experiment. System is approximately 2.5 m in length from source (back center) to shoreline. Topographic measurements were taken along laser sheet line located 1.75 m from sediment source.

the shoreline to be maintained at an approximately constant location through the course of the experiment. A photograph of the experimental set-up is shown in Figure 3. *Sheets et al.* [2007] used a sediment mixture of 70% 120 μm silica sand and 30% bimodal (190 μm and 460 μm) anthracite coal.

[12] Topographic measurements were taken following a well established protocol prototyped at the Experimental Earthscape Basin (XES) using a sub-aerial laser topography scanning system [*Sheets et al.*, 2002]. Unlike the XES system, however, where the topography of the entire fluvial surface is mapped periodically, topography was monitored at 2 min intervals along a flow-perpendicular transect located 1.75 m from the infeed point. A time series of

deposition along this transect is shown in Figure 4. This system provided measurements with a data-sampling interval of 0.8 mm in the horizontal and with a measurement precision of 0.9 mm in the vertical. The experiment lasted 30 h and produced an average of 0.2 m of stratigraphy. Upon completion of the experiment, the deposit was sectioned and imaged at the topographic strike transect. This allows direct comparison of the preserved stratigraphy to the elevation increments that generated the stratigraphy.

[13] No attempt was made to formally scale the results from this experiment to field scale, nor were the experimental parameters set to produce an analog to any particular field case. Rather, the goal of the experiment was to create a self-organized, distributary depositional system in which many of the processes characteristic of larger depositional channel systems could be monitored in detail over spatial and temporal scales which are impossible to obtain in the field. The rationale for such experiments is discussed in detail by *Paola et al.* [2009]. As discussed earlier, the focus of the present study is on identifying the general class of distributions (i.e., heavy versus thin tail) that characterize the kinematics of topography in the DB-03 experiment and explore their relationship to the architecture of the preserved stratigraphy.

2.2. Definitions and Data Analysis

[14] At any spatial location on the topographic line where elevation was monitored (see Figure 5) we define elevation increments in time as:

$$\delta h_i(t) = h(t + \Delta t) - h(t) \qquad (1)$$

Where $h(t)$ is the elevation at time t at a given location and Δt is the temporal resolution of the experimental data. We recognize positive values of elevation increments as magnitudes of deposition and negative values as magnitudes of erosion:

$$D_i = \delta h_i(t) > 0 \qquad (2a)$$

$$E_i = \delta h_i(t) < 0 \qquad (2b)$$

It is worth noting that the general form of (2a) and (2b) does not distinguish between deposition and erosion related to sediment dynamics versus tectonic environment. Let us now define the durations of continuous deposition, t_d, as uninterrupted periods for which $\delta h_i(t) > 0$, and the durations of erosional events, t_e, as uninterrupted periods for which $\delta h_i(t) < 0$. Further, let us define the magnitude of the depositional (D_e) and erosional events (E_e), collectively denoted by $\delta h_e(t)$, as the sum of all the elevation increments over a duration where the sign of $\delta h_i(t)$ remains unchanged, that is, the depositional events D_e and erosional events E_e are defined as:

$$D_e = \sum_{i=1}^{t_d} D_i \qquad (3a)$$

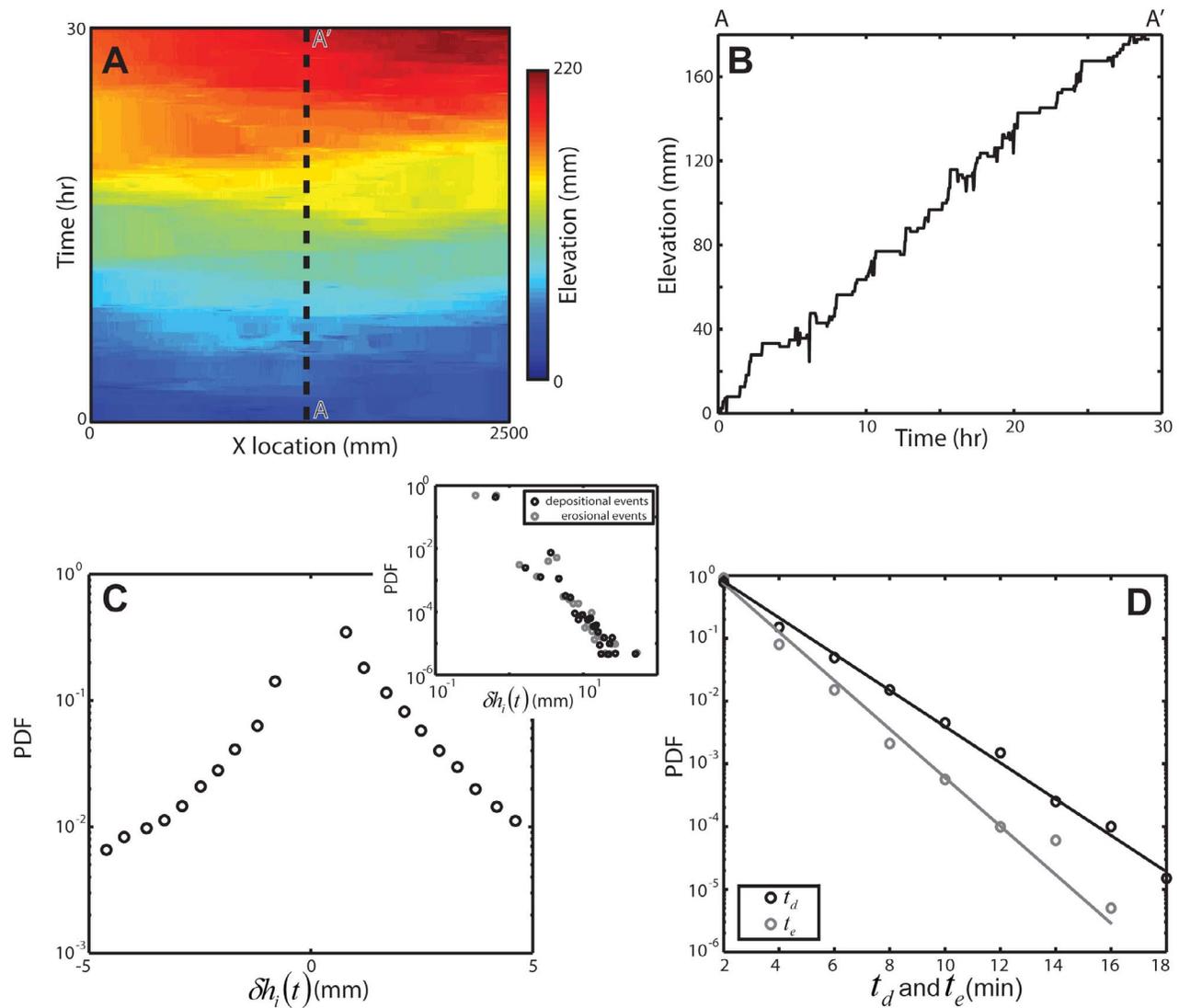$$E_e = \sum_{i=1}^{t_e} E_i \qquad (3b)$$

Figure 4. Data defining evolution of topography and surface dynamics calculated from topographic surveys for the DB-03 experiment along a transect oriented approximately perpendicular to the dominant flow direction, 1.75 m from infeed point. (a) Space time plot of sequential delta-top profiles shown every 120 s. (b) Example of time series of topography measured at a single location, roughly located in the center of the topographic survey. (c) PDF of $\delta h_i(t)$ shown in both semi-log and log-log plots. PDF built from ensemble of all time transects in Figure 4a. Linear decay of depositional and erosional increments in log-log space suggests power law distribution. (d) PDFs of t_d and t_e shown in semi-log plots. Linear decay of durations of deposition and erosion in semi-log space suggest thin-tailed distribution.

collectively denoted as:

$$\delta h_e(t) = \{D_e, E_e\} \qquad (4)$$

It is noted that the magnitudes of depositional and erosional events as defined above can be seen as derived variables that result as the random sums of random variables. Finally, as in the *Kolmogorov* [1951] analysis, the bed thickness, D_{st}, is defined as the sediment thickness between two successive preserved surfaces of erosion. Figures 1 and 5 illustrate the definition of random variables ($\delta h_i(t), D_e, E_e, t_d, t_e, \delta h_e(t), D_{st}$).

The statistical characteristics of these random variables are examined in the next section.

3. Experimental Results

[15] In this section we summarize the statistics that characterize the surface dynamics of the DB-03 experiment [see also *Ganti et al.*, 2011] and also provide a detailed statistical characterization of the thicknesses of beds of both the constructed stratigraphy (using the surface elevation series) and the physical stratigraphy (extracted from the preserved stratigraphic sections) that resulted from this experiment. All the statistics presented in section 3 were computed on the
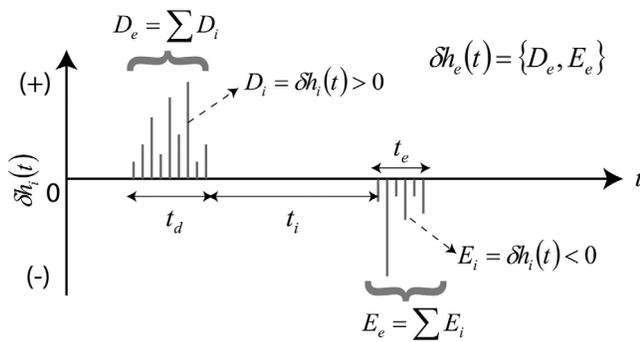
Figure 5. Schematic diagram illustrating the variables and time-sequence of events associated with constructing a stratigraphic bed. Deposition that follows an erosional event occurs as a sequence of continuous depositional increments, D_i, over a duration, t_d. Combined these depositional increments make up a depositional event, D_e. Either immediately following this deposition, or after some duration of inactivity, t_i, a sequence of continuous erosional increments, E_i, over duration, t_e, occur. Combined these erosional increments make up an erosional event, E_e.

ensemble of time series along the topographic transect referenced in Figure 3 and the total number of time transects available was 2502, each for a duration of 30 h.

3.1. Statistics of Surface Evolution

[16] Using the definition of elevation increments, $\delta h_i(t)$ (equation (1)), we constructed a probability density function (PDF) of all increments at each measurement location along the transect at $x = 1.75$ m (Figure 3). Figure 4c shows the empirical PDF for these data in both semi-log and log-log plots. The concave up nature of both the positive and negative elevation increments in the semi-log plot and the linear decay of both depositional and erosional increments in the log-log plot suggest that the magnitudes of deposition and erosion (D_i and E_i), are best characterized by heavy-tailed (power law) statistics. In contrast to thin-tailed PDFs, where the chance of occurrence of an extreme event is vanishingly small, in heavy-tailed PDFs an extreme event has a small but significant chance of occurrence. Heavy-tailed PDFs have a power law decay which is a slower decay than exponential. In most natural processes, system constraints impose an upper bound in the values of the variables of interest and require the need for the use of truncated power law distributions. Such a distribution is the truncated Pareto distribution defined as:

$$f(x) = \frac{\alpha \gamma^\alpha x^{-\alpha-1}}{1 - (\gamma/\upsilon)^\alpha} \qquad (5)$$

Where υ is the truncation parameter or the upper bound on the random variable, α is the tail index, and γ is the lower bound on the random variable x. The tail index α quantifies the probability of extreme events with a smaller value of α indicating a heavier tail and thus a higher chance of an extreme event. *Ganti et al.* [2011] reported that the truncated Pareto distribution provides a good fit to the experimental data of magnitudes of deposition and erosion, D_i and E_i, with estimated tail parameters $\hat{\alpha}_1 = 2.41$ and $\hat{\alpha}_2 = 1.1$, respectively. The estimated upper bound for both of these PDFs

was found to be 35 mm, coinciding with the independently estimated approximate maximum channel depth measured during this experiment, and the estimated lower bounds were found to be $\hat{\gamma}_1 = 2.0$ mm and $\hat{\gamma}_2 = 0.3$ mm, respectively, for magnitudes of deposition and erosion.

[17] The durations of the depositional and erosional events, t_d and t_e, respectively, were computed from the surface elevation increment series and their PDFs are presented in Figure 4d. Unlike the elevation increments that were found to exhibit heavy-tails, the durations of deposition and erosion exhibit thin-tailed PDFs and were well approximated by an exponential distribution:

$$f(x) = \lambda e^{-x\lambda} \qquad (6)$$

Where λ is the decay rate parameter, which is also equal to the inverse of the distribution's mean. The scale parameters that gave the best fits for the PDFs of the durations of deposition and erosion were $\frac{1}{\lambda_{t_d}} = 2.6$ min and $\frac{1}{\lambda_{t_e}} = 2.2$ min, respectively. The observation that the estimated means of durations of depositional and erosional events are only slightly greater than the sampling resolution of our data (2 min) suggests that some alternations between erosion and deposition and vice versa that occurred in our experiment at scales smaller than the recording interval of 2 min might not have been captured in our elevation time series. This is a direct consequence of the documented multifractal structure of the surface elevation evolution of the deltaic surface [*Ganti et al.*, 2011]. It was shown in that study that the zeros (periods of inactivity) in the series of elevation increments are present at all scales, which implies that the alternations between erosion to inactivity or deposition to inactivity and vice versa, would occur at all scales of observation of the system. Thus, this forces the estimation of statistics of durations of depositional and erosional events to be scale-dependent. It is important to note that though the statistical structure of the length of zeros (periods of inactivity) in the elevation increments imply a scale-dependent estimated time statistics, it does not affect the preserved bed thicknesses as the periods of inactivity do not contribute to the creation of a stratigraphic column.

[18] Taken together, the random variables D_i, E_i, t_d, and t_e are sufficient to estimate the magnitudes of depositional and erosional events, D_e and E_e respectively (using equation (3a) and (3b)). Combined, these random sums of elevation increments, when the vertical extents of both continuous erosional and depositional events are treated separately, form $\delta h_e(t)$ (see equation (4)) as defined by *Kolmogorov* [1951]. However, while Kolmogorov assumed a Gaussian distribution for $\delta h_e(t)$), *Ganti et al.* [2011] found that the PDFs of depositional and erosional events, D_e and E_e (which together form $\delta h_e(t)$), are well fit by truncated Pareto distributions. The tail indices of the best fit truncated Pareto distributions for depositional and erosional events were $\hat{\alpha}_1' = 3.3$ and $\hat{\alpha}_2' = 3.0$, respectively. We can see that the distributions of depositional and erosional events have thinner tails (higher tail indexes or faster decay) than their parent distributions, D_i and E_i, respectively. The tail thinning effect during the conversion of elevation increments $\delta h_i(t)$ to depositional and erosional events $\delta h_e(t)$ is expected as a result of weak convergence of truncated heavy-tailed random variables to
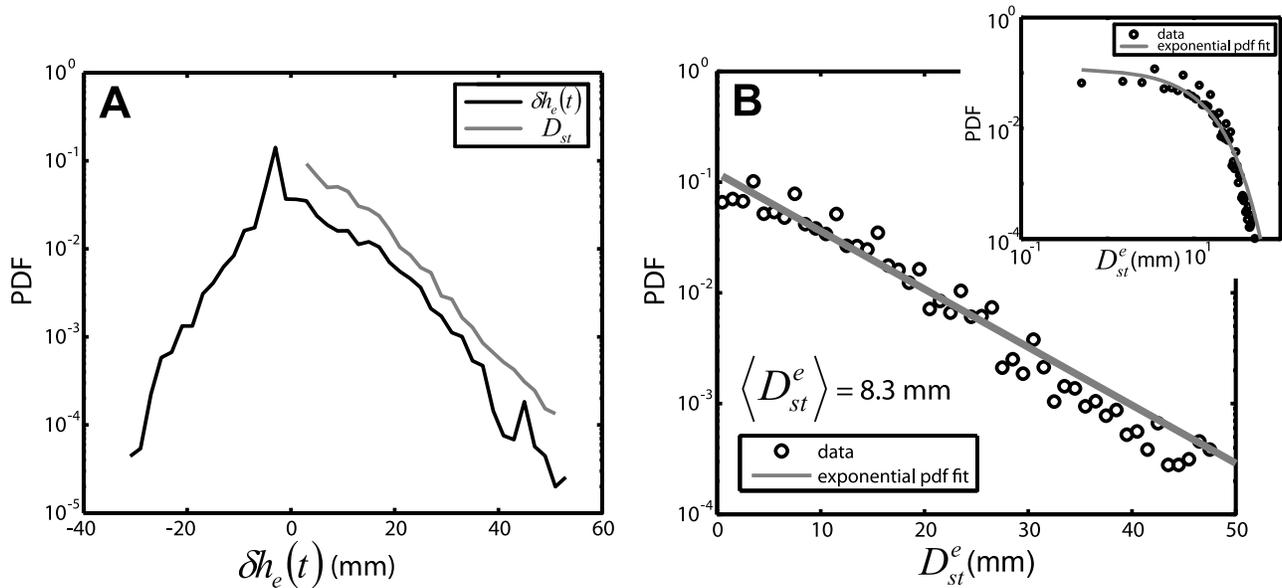
Figure 6. Data defining evolution of topography and resulting synthetic stratigraphy calculated from topographic surveys for the DB-03 experiment along a transect that is oriented approximately perpendicular to the dominant flow direction, 1.75 m from infeed point. (a) Comparison of the distributions of Kolmogorov events, $\delta h_e(t)$, and resulting bed thicknesses. (b) PDF of D_{st}^e shown in both semi-log and log-log plots. Linear decay of bed thicknesses in semi-log space suggests exponential distribution.

the Central Limit Theorem, in effect filtering out some of the heavy-tailed surface evolution statistics.

3.2. Statistics of Preserved Stratigraphy

[19] The thickness of beds preserved in the stratigraphic columns was calculated in two different ways: 1) constructed from the topographic data collected during the experiment (termed D_{st}^e), and 2) directly measured from the digital images of the preserved stratigraphy available after sectioning the final deposit (termed D_{st}^s). A comparison of the statistics of these two independently estimated variables tests the degree to which our definition of a bed as a package of sediment bounded by erosional surfaces translates to features readily identifiable by textural changes in the deposit.

[20] Bed thicknesses, D_{st}^e, were constructed from the elevation measurements as outlined schematically in Figure 1. At each spatial location, the elevations of all preserved erosional boundaries were first identified and then the thicknesses of sediment bounded by those preserved erosional surfaces were calculated. The probability density function of the preserved bed thickness, D_{st}^e, in both semi-log and log-log plots is shown in Figure 6b. Unlike the increments of deposition and erosion discussed above, the thickness of beds exhibits a thin-tailed PDF. Figure 6b shows that an exponential distribution with mean $\langle D_{st}^e \rangle = 8.3$ mm provides a good fit to the calculated bed thicknesses.

[21] Bed thicknesses, D_{st}^s, were computed from the images of preserved stratigraphy using the high optical contrast between the white quartz grains and black anthracite grains. The difference in density (quartz: 2650 kg/m^3 versus anthracite: 1700 kg/m^3) results in differences in their relative mobility, that is, the lighter anthracite particles tend to be more mobile than the quartz grains and are therefore a proxy

for fine sediment. This difference in mobility is recorded in the deposit where the coal and quartz often form distinct depositional bodies, such as channel fills and lobes [*Sheets et al.*, 2007], and develop textural boundaries between white and black sediment which can be used as bed boundaries. Using undistorted images of the physical stratigraphy (Figure 7a) we generated stratigraphic panels with a binary identification scheme. Using a threshold luminosity value we separated anthracite deposits from quartz deposits. The threshold value used for this operation was picked by identifying a value that on visual inspection appeared to correctly separate the deposit types. Using these binary images (Figure 7b) we measured bed thicknesses from the stratigraphy, D_{st}^s, as uninterrupted vertical sequences of pixels of a single grain type (i.e., either only white or only black). The probability density function of preserved bed thickness, D_{st}^s, is shown in semi-log space in Figure 7c. Similar to the PDF of D_{st}^e estimated from the surface elevation measurements, the PDF of D_{st}^s estimated from the physical stratigraphy is close to exponential with an estimated mean, $\langle D_{st}^s \rangle$, of 9.5 mm. Importantly, we note that the two distributions of bed thickness, one theoretical, and one measured, both demonstrate that the heavy-tailed statistics of deposition and erosion that characterize the surface evolution are not preserved in the stratigraphy.

[22] We emphasize that the theory of *Kolmogorov* [1951] used the surface elevation time series to construct the preserved bed thicknesses. This is not the same as extracting bed thicknesses from physical stratigraphy as the observable stratal boundaries are not exactly equivalent to the definition of bed boundaries as defined by *Kolmogorov* [1951]: not all visible stratal boundaries are erosional, and not all erosional boundaries result in a change of sediment type. Rather, the boundaries we mapped represent a straightforward class of
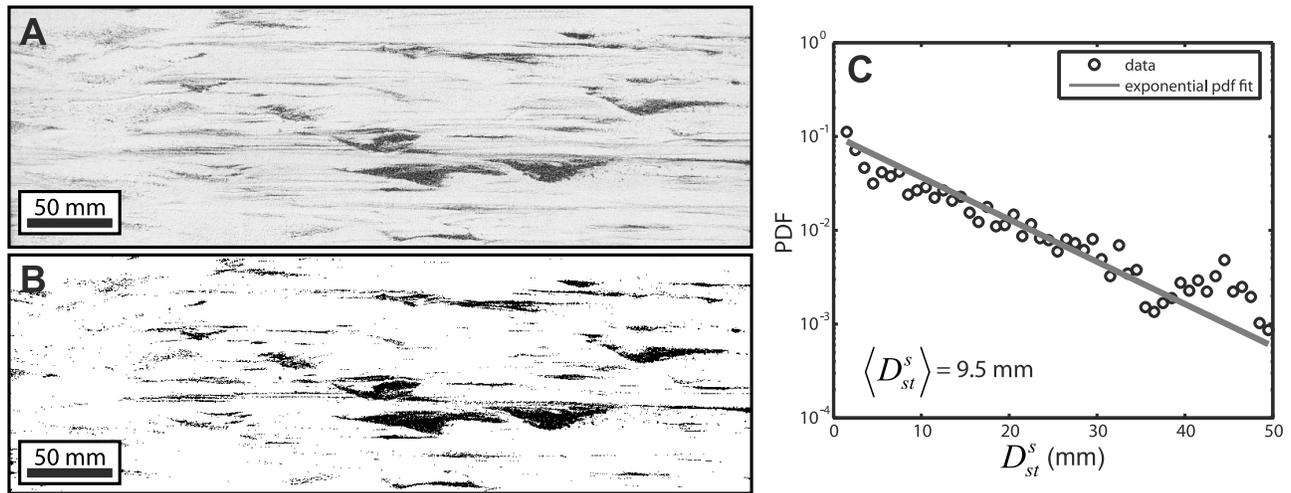
Figure 7. Information defining distribution of bed thicknesses for DB-03 experiment generated from images of physical stratigraphy. (a) Photograph of approximately 0.14 m of stratigraphy generated during DB-03 experiment. Stratigraphic section is located approximately 1.75 m from source. (b) Facies map of stratigraphy where white pixels represent quartz deposits and black pixels represent coal deposits. Quartz and coal deposits were identified through threshold luminosity analysis outlined in section 4.2. (c) PDF of D_{st}^s shown in semi-log space generated from deposit facies map. Linear decay of bed thicknesses in semi-log space suggests exponential distribution.

bed boundaries one might map in the field. A pleasing result of our analysis is the agreement between the constructed and physical stratigraphy statistics giving more confidence in applying the analytical results of *Kolmogorov* [1951] and other studies which use elevation series to define preserved bed thickness. In the next section we use stratigraphic columns synthetically generated from different families of parent distributions for elevation increments to explore the generality of the experimental results and also to explore the connection between surface evolution statistics and preserved stratigraphy statistics in different scenarios.

4. Results From Stochastic Sedimentation Models

4.1. Stochastic Models of Surface Elevation Evolution

[23] The analysis of surface morphodynamics and the preserved stratigraphy statistics presented in the previous section suggest that heavy-tailed distributions of surface evolution do not necessarily translate to heavy-tailed distributions of bed thickness in strata. How general is this result, and are there conditions in which heavy-tails in surface elevation increments can be transferred into the stratigraphic record? We explore these questions using a series of stratigraphic columns constructed from stochastically generated surfaces of sedimentation and erosion (referred to as "synthetic stratigraphic columns"). Several studies have explored the relationship between stochastic models for surface evolution and the synthetic stratigraphy that they generate [*Molchan and Turcotte*, 2002; *Muto*, 1995; *Pelletier and Turcotte*, 1997; *Schwarzacher*, 1975; *Strauss and Sadler*, 1989], but no study, to the best of our knowledge, has quantified the effect of heavy-tailed surface elevation increments on the preserved stratigraphy. The advantages of constructing preserved stratigraphic columns from stochastically generated surface elevation series include the ability to

explore many physical scenarios for which data are not available and the ability to produce long time series where the shapes of resulting distributions can be confidently interpreted. Such analyses allow us to examine the generality and validity of inferences made from our experimental discretely sampled elevation time series.

[24] We use a 1D model of erosion and sedimentation based on a random-walk formulation that assumes independent magnitudes of erosion and deposition. The magnitudes of erosion and deposition, $\delta h_i(t)$, are assumed to be sampled from a symmetric distribution with thin- or heavy-tails. Specifically, given the concentrated mass at zero (significant chance of having zero or close to zero magnitudes) found from the analysis of experimental data [see also *Ganti et al.*, 2011] we assume that the surface elevation increments, δh_i, come from either a Laplace distribution (in the case of thin-tails) or a double Pareto distribution (in the case of heavy-tails). The Laplace distribution, also called a double exponential distribution, is given by

$$f(\delta h_i) = \frac{1}{2b} e^{\left(-\frac{|\delta h_i - \mu|}{b}\right)} \tag{7}$$

Where b is the scale parameter of the distribution and μ is the location parameter (or the mean of the distribution). The double Pareto distribution is given by

$$f(\delta h_i) = \alpha \frac{\mu^\alpha}{\delta h_i^{\alpha+1}}; \text{ when } \delta h_i \geq \mu \tag{8a}$$

$$f(\delta h_i) = \alpha \frac{\mu^\alpha}{2(2\mu - \delta h_i)^{\alpha+1}} \text{ when } \delta h_i < \mu \tag{8b}$$

where μ is the mean of the distribution and α is the tail-index.
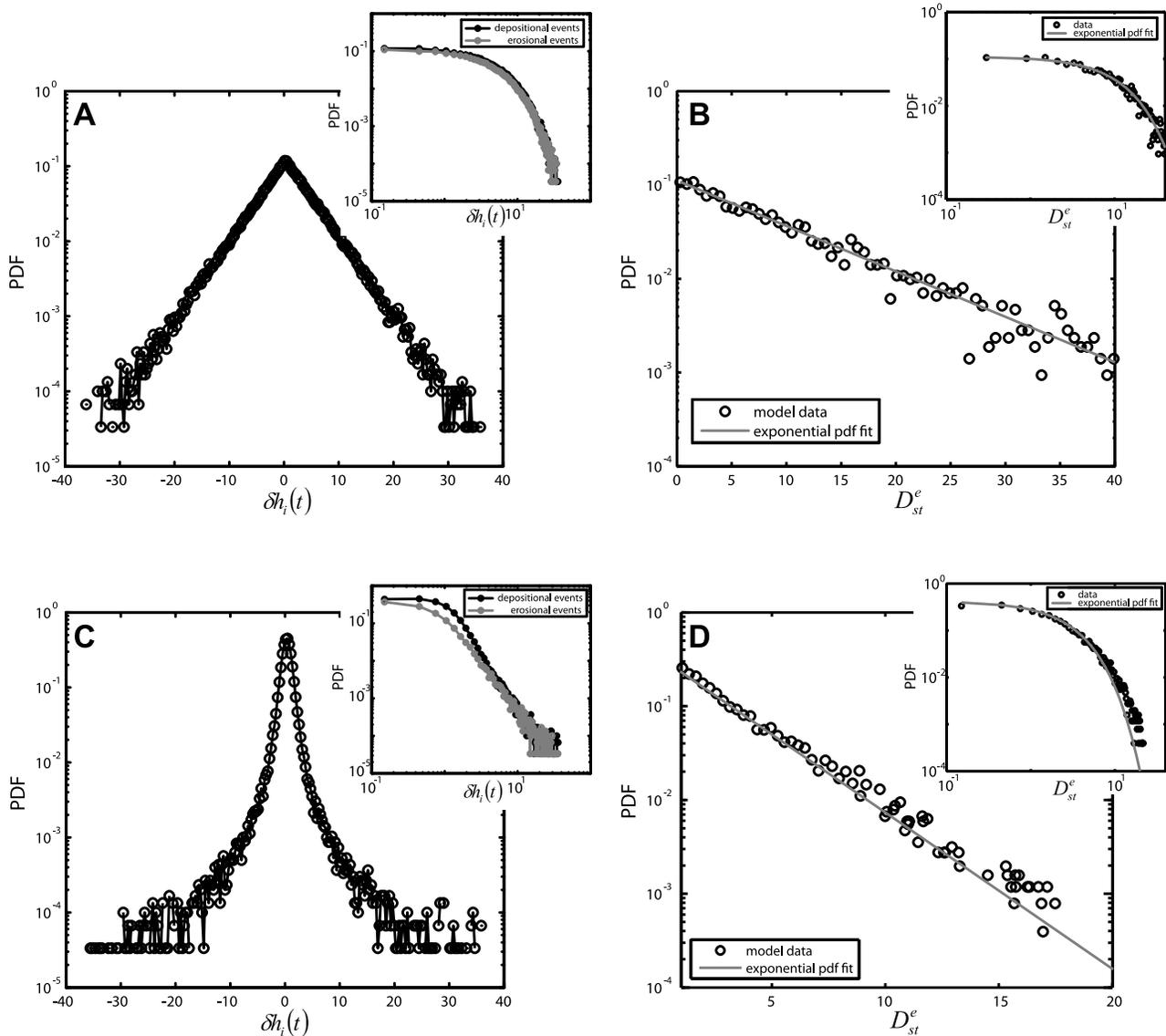
Figure 8. Comparison of results from (a, b) 1D numerical models of surface evolution and resulting stratigraphy associated with exponentially distributed elevation fluctuations and (c, d) power law distributed elevation fluctuations. (Figure 8a) Input PDF of $\delta h_i(t)$ generated from a Laplace distribution of elevation fluctuations with $b = 4.1$ and $\mu = 0.3$. (Figure 8b) PDF of D_{st}^e shown in both semi-log and log-log plots. Linear decay of bed thicknesses in semi-log space suggests exponential distribution. (Figure 8c) Input PDF of $\delta h_i(t)$ generated from a double Pareto distribution of mean = 0.3 and $\alpha = 1.5$. (Figure 8d) PDF of D_{st}^e shown in both semi-log and log-log plots. Linear decay of bed thicknesses in semi-log space suggests exponential distribution. Distributions for both scenarios were generated from model time series with 100,000 elevation increments.

[25] After generating time series of elevation increments resulting from the above two 1D random-walk models, local preserved minima can be identified and bed thicknesses calculated. A summary of the statistics of preserved stratigraphic columns constructed from the stochastically generated surface elevation series is presented in the next subsection.

4.2. Statistics of the Constructed Stratigraphic Columns

[26] As a first step in quantifying the relationship between a parent distribution of elevation increments, $\delta h_i(t)$, and

preserved bed thicknesses, D_{st}, we compare the distribution of beds constructed from symmetric, positive mean, thin-tailed distributions of elevation increments (equation (7)) to those constructed from symmetric, positive mean, heavy-tailed distributions of elevation increments (equation (8)) for a range of parameters of these distributions. Examples of the distributions of $\delta h_i(t)$, D_{st}, t_d, t_e, $\delta h_e(t)$ associated with our thin-tailed and heavy-tailed elevation increments are shown in Figures 8 and 9. For all scenarios explored, we find that: (1) the distribution of Kolmogorov events, $\delta h_e(t)$, show an exponential-type of decay in their tails (thin-tailed) irrespective of the nature of the distribution of elevation
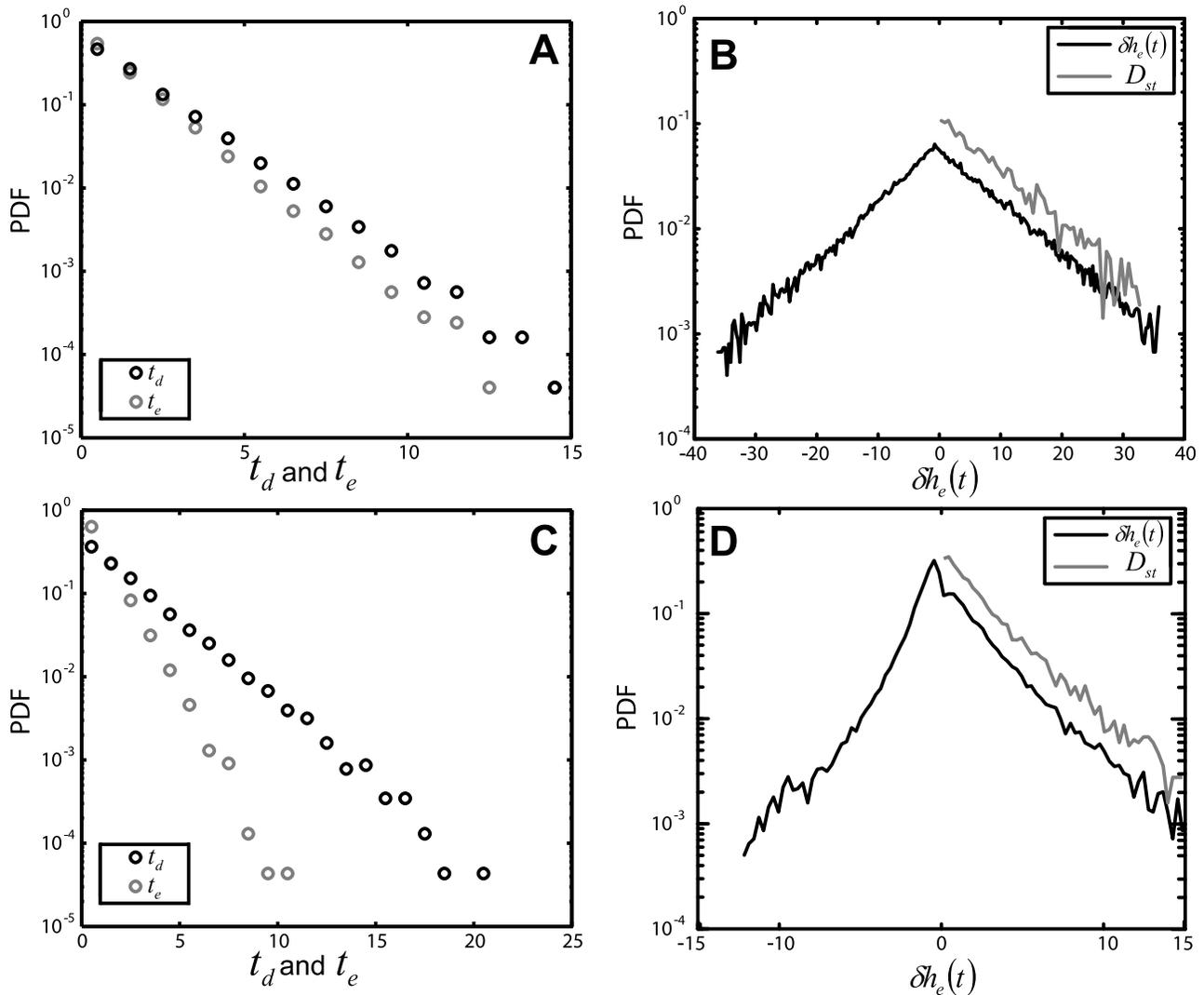
Figure 9. Comparison of results from (a, b) 1D numerical models of surface evolution and resulting stratigraphy associated with exponentially distributed elevation fluctuations and (c, d) power law distributed elevation fluctuations. (Figure 9a) PDF of t_d and t_e shown in semi-log space and generated from distribution of elevation increments presented in Figure 8a. (Figure 9b) Distribution of Kolmogorov elevation events, $\delta h_e(t)$, and resulting bed thicknesses, D_{st}^e. (Figure 9c) PDF of t_d and t_e shown in semi-log space and generated from distribution of elevation increments presented in Figure 8c. (Figure 9d) Distribution of Kolmogorov elevation events, $\delta h_e(t)$, and resulting bed thicknesses, D_{st}^e.

increments, $\delta h_i(t)$ (Figures 9b and 9d), (2) the distributions of durations of depositional and erosional events (t_d and t_e) are always well approximated by thin-tailed distributions, and (3) the resulting bed thicknesses, D_{st}, are best described by exponential distributions (Figures 8b and 8d). The outcome of our numerical experiments shows specifically how the process of constructing stratigraphic beds from elevation fluctuations in net depositional settings is associated with a filtering of the information contained within the tails of elevation increments distributions.

5. Discussion

[27] As was shown in the previous section, the heavy-tailed statistics of surface evolution do not always get preserved in the bed thickness statistics. In this section, we will probe further into how the interplay between the probabilistic structure (i.e., thin-tailed versus heavy-tailed) of the magnitudes of deposition and erosion and the durations of depositional and erosional events effect the distribution of preserved bed thickness. In the remainder of the manuscript, for the simplicity of notation, we denote any two random variables to have a symmetric distribution if they have the same nature of decay in their tails (i.e., exponential, thin-tailed versus power law, heavy-tailed).

5.1. Influence of Symmetry of the Topographic PDF

[28] An interesting characteristic of both the experimental data and the stochastic surface elevation models described so far is the symmetrical nature of the distributions of the erosional and depositional events, $\delta h_e(t)$, and the durations of depositional and erosional events, t_d and t_e. To analyze the

importance of this symmetry for the resulting distributions of bed thicknesses, we compare distributions of bed thickness that result from symmetrical and asymmetrical parent distributions of magnitudes of deposition and erosion. In this exercise, rather than constructing synthetic stratigraphic columns from random-walk models of surface elevation increments, we directly generate beds using the difference between the two random variables, depositional events (D_e) and erosional events (E_e), which are in effect random sums of elevation increments, D_i and E_i:

$$\hat{D}^e_{st} = \sum_{i=1}^{t_d} D_i - \sum_{i=1}^{t_e} E_i \qquad (9)$$

It is worth noting that the bed thicknesses calculated using equation (9) are an approximation of the bed thicknesses constructed from the surface evolution, as this equation takes into account only the erosional thinning of depositional events by the next subsequent erosional event, and not the erosional thinning that could possibly occur due to large magnitude events that could have occurred later in a time series. While equation (9) produces only an approximation of bed thickness distributions resulting from a random-walk model of surface elevation evolution, the advantage of using it is that it allows independent control of the distributions of D_i, E_i, t_d, and t_e. In this subsection, we investigate the influence of the symmetric versus asymmetric nature of the distribution of elevation increments and the distributions of the durations of depositional and erosional events on the resulting bed thickness distribution. First, we use equation (9) to generate distributions of bed thickness for scenarios in which both elevation increments, $\delta h_i(t)$, and the durations of depositional and erosional events, t_d and t_e, have symmetrical distributions, as has been the case for our experimental data and the numerical simulations. Our simulation results demonstrate that, regardless of the shape of the input distributions for $\delta h_i(t)$ and t_d, t_e (i.e., thin-tailed versus heavy-tailed), the bed thickness distributions computed using equation (9) are exponentially distributed so long as the parent distributions are symmetrical. An example of this is shown in Figure 10b where we generated the random variables D_i and E_i from symmetric Pareto distributions and generated the random variables t_d and t_e from symmetrical exponential distributions.

[29] Next we examine the influence of asymmetry in the distributions of D_i and E_i on the resulting distribution of bed thickness while keeping the t_d and t_e distributions symmetrical. Interestingly, as the asymmetry of the D_i to E_i distributions increases, the resulting distribution of bed thickness becomes increasingly weighted toward extremes (approaches a power law in shape). An extreme example of this finding is shown in Figure 10c where we generated magnitudes of deposition, D_i, from a Pareto distribution with a tail index of 0.75 (very heavy-tail) while generating magnitudes of erosion, E_i, values from an exponential distribution with a scale parameter equal to 5 and the durations of depositional and erosional events from exponential distributions with a scale parameter of 10. The result is a heavy-tailed bed thickness distribution. We assert that this observation represents an important clue as to why bed thickness distributions generated from heavy-tailed surface increments are

often exponentially distributed. In systems with heavy-tailed surface increments that have a symmetric distribution, the heavy-tails from one side of the distribution (erosional events) effectively cancel out the heavy-tails from the other side of the distribution (depositional events), thus resulting in a derived distribution that is thin-tailed. Alternatively, increasing the asymmetry of the parent distribution reduces the ability for large magnitude but infrequent erosional increments to balance out large magnitude but infrequent depositional increments, therefore leading to heavy-tailed bed thickness distributions.

[30] In both the experimental data set and the stochastic surface elevation models we find that the durations of depositional and erosional events are well described by thin-tailed distributions. We do not prescribe t_d and t_e in our 1D stochastic surface elevation models, but rather they are determined by our assumption of independence between magnitudes of deposition and erosion $\delta h_i(t)$ (can be shown theoretically to follow a negative Binomial distribution). With this information in mind, we explore the implications of asymmetry in the distributions of t_d and t_e. Similar to the effect of increasing the asymmetry of the $\delta h_i(t)$ distribution, we find that as the asymmetry of t_d to t_e distributions increases, the resulting distribution of bed thicknesses has more weight in the extremes (approaches power law in shape). An extreme example of this is shown in Figure 10d where we sampled durations of depositional events, t_d, from a Pareto distribution with a tail index of 1.75 while sampling the durations of erosional events, t_e, from an exponential distribution with a scale parameter equal to 10 and magnitudes of deposition and erosion from symmetrical Pareto distributions with a tail index of 1.5. In Table 1 we summarize our observations on the link between symmetry in the distributions that describe the surface dynamics and the resulting shape of the bed thickness distribution.

[31] Finally, to test the accuracy of the approximation used in equation (9) to describe the preserved bed thicknesses, we generated random variables D_i, E_i, t_d, and t_e using distributions that described the surface evolution in the DB-03 experiment. We used Pareto distributions for D_i and E_i with tail indexes α_1 and α_2 equal to 2.6 and 1.1, respectively and exponential distributions for t_d and t_e with $\langle t_d \rangle = 2.6$ min and $\langle t_e \rangle = 2.2$ min. The bed thicknesses calculated using these parameters was found to be well approximated by an exponential distribution, with $\left\langle \hat{D}^e_{st} \right\rangle$ of 6.2 mm, slightly less than the value we estimated for the DB-03 experiment (Figure 10a). This agreement confirms the validity of our stochastic simulations for the purpose of studying how the interplay between depositional and erosional events gets recorded in the preserved stratigraphy.

5.2. Mapping Surface Variability to Bed-Thickness Statistics

[32] In Sections 3.2, 4 and 5.1, we presented data from physical and numerical experiments that indicate that the statistics describing the preserved bed thicknesses generally do not record the signature of heavy-tailed surface evolution statistics. While information on the nature of the distribution's tail (thin-tailed versus heavy-tailed) of surface evolution events may be filtered from the stratigraphic record, in this section we demonstrate variability of elevation
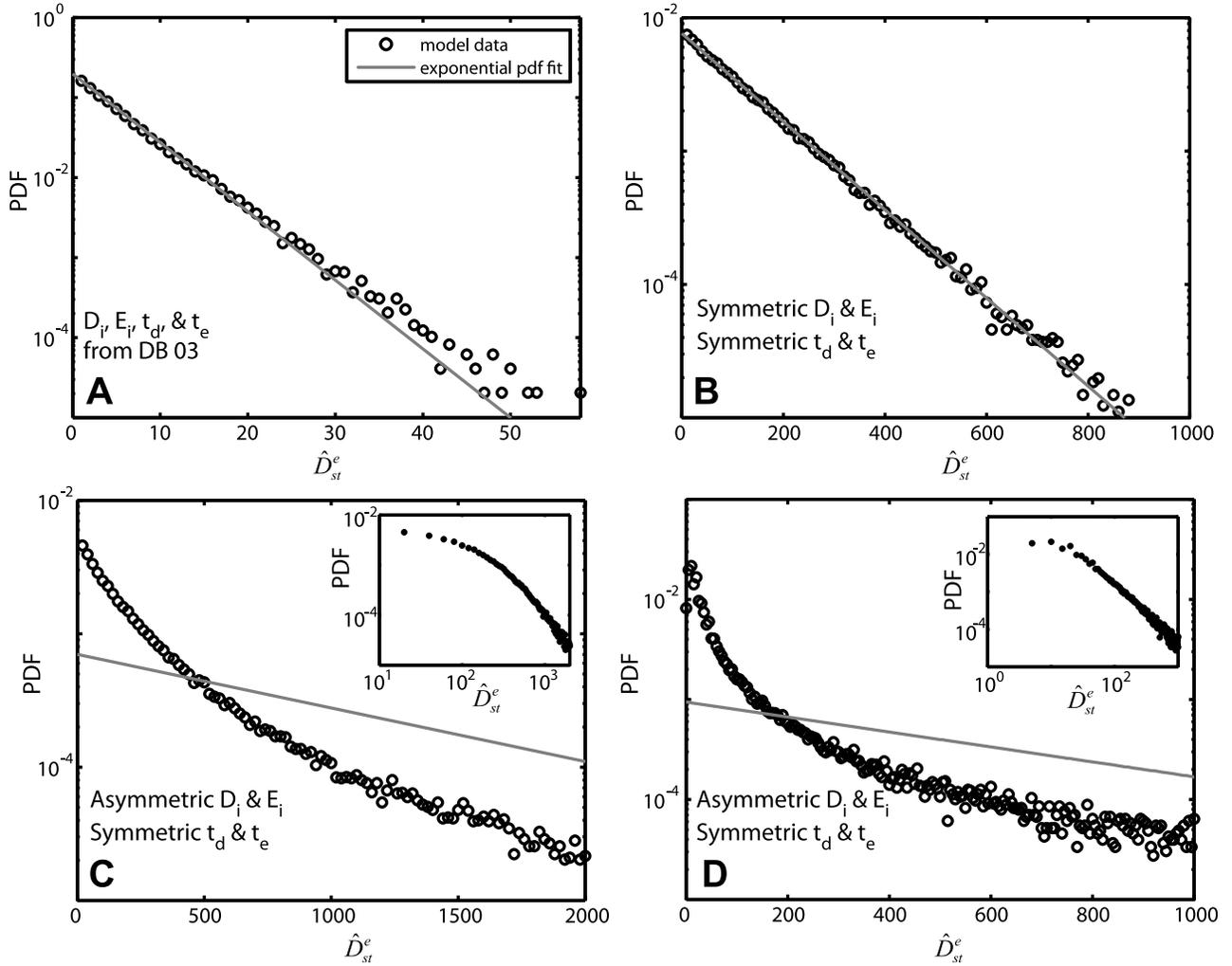
Figure 10. Bed thickness distributions generated from individual bed thicknesses calculated using equation 9. (a) PDF of bed thicknesses generated using equation 9 with input parameters for D_i, E_i, t_d and t_e set to equal estimated parameters from DB-03 experiment. (b) PDF of bed thicknesses generated from symmetric distributions of both D_i/E_i and t_d/t_e. Random values of D_i and E_i are described by a Pareto distribution with tail-index of 1.5. Mean of combined distribution of depositional and erosional increments, $\delta h_i(t)$ is 10. Random values of t_d and t_e are described by an exponential distribution with mean of 10. (c) PDF of bed thicknesses generated from asymmetric distribution of D_i/E_i and symmetric distribution of t_d/t_e. Random values of D_i are described by a Pareto distribution with tail-index of 0.75 while values of E_i are described by an exponential distribution with $1/\lambda = 5$. Mean of combined distribution of depositional and erosional increments, $\delta h_i(t)$ is 10. Random values of t_d and t_e are described by an exponential distribution with $1/\lambda$ of 10. (d) PDF of bed thicknesses generated from symmetric distribution of D_i/E_i and asymmetric distribution of t_d/t_e. Random values of D_i and E_i are described by a Pareto distribution with tail-index of 1.5. Mean of combined distribution of depositional and erosional increments, $\delta h_i(t)$ is 10. Random values of t_d are described by a Pareto distribution with tail-index of 1.75 while values of t_e are described by an exponential distribution with μ of 10.

increments, δh_i, relative to the mean deposition, $\langle \delta h_i \rangle$, influences the mean of preserved bed thicknesses, $\langle D_{st} \rangle$. This was demonstrated analytically by *Paola and Borgman* [1991] for the case of zero net deposition and thin-tailed elevation statistics; here we generalize that result. Specifically, we are interested in relating the variability and mean of elevation increment distributions to the statistics describing the preserved bed thicknesses. One common measure of a distribution's variability is the interquartile range, *IQR*, which is equal to the difference between the third and first quartiles of the distribution. To compare the spread of the parent distribution to its mean we examine the nondimensional interquartile range coefficient, $\Phi_{\delta h_i}$:

$$\Phi_{\delta h_i} = \frac{IQR_{\delta h_i}}{\langle \delta h_i \rangle} = \frac{F_{\delta h_i}^{-1}(0.75) - F_{\delta h_i}^{-1}(0.25)}{\langle \delta h_i \rangle} \tag{10}$$

Table 1. Regime Matrix Illustrating Relationship Between Shape of D_i, E_i, t_d, and t_e Distributions and Resulting D_{st} Distribution

		Asymmetric D_i and E_i Distributions		
	Symmetric D_i and E_i Distributions	Both Distributions are Thin-Tailed	Both Distributions are Heavy-Tailed	D_i Distributions Heavy-Tailed, E_i Distribution Thin-Tailed
Symmetric t_d and t_e Distributions	D_{st}: Thin-tailed	D_{st}: Thin-tailed	D_{st}: Between thin and heavy-tailed	D_{st}: Heavy-tailed
Asymmetric t_d and t_e distributions. Both distributions are thin-tailed	D_{st}: Thin-tailed	D_{st}: Thin-tailed	D_{st}: Between thin and heavy-tailed	D_{st}: Heavy-tailed
Asymmetric t_d and t_e distributions. Both distributions are heavy-tailed	D_{st}: Between thin and heavy-tailed	D_{st}: Between thin and heavy-tailed	D_{st}: Between thin and heavy-tailed	D_{st}: Heavy-tailed
Asymmetric t_d and t_e distributions. t_d distributions heavy-tailed, t_e distribution thin-tailed.	D_{st}: Heavy-tailed	D_{st}: Heavy-tailed	D_{st}: Heavy-tailed	D_{st}: Heavy-tailed

An additional metric that compares a distribution's variability to its mean is the coefficient of variation, $CV_{\delta h_i}$, defined as:

$$CV_{\delta h_i} = \frac{\left\langle (\delta h_i - \langle \delta h_i \rangle)^2 \right\rangle^{1/2}}{\langle \delta h_i \rangle} \qquad (11)$$

An advantage of the interquartile range over the coefficient of variation is that the interquartile range of all thin-tailed and heavy-tailed distributions formally exists, while the standard deviation, σ, does not formally exist for heavy-tailed distributions with a tail index less than 2. We note, though, that for any finite sequence of random numbers generated from a thin or heavy-tailed distribution, a standard deviation can always be calculated. However, for thin-tailed random variables, the calculated standard deviation converges to a fixed value with an increase in the sample size while, for heavy-tailed random variables with tail index less than 2, the calculated standard deviation diverges with increasing sample size, casting uncertainty in inferences from finite size data sets. With this in mind, we generated a sequence of synthetic stratigraphic columns, as outlined in section 5.1, constructed from elevation increments that span a range of values of the non-dimensional interquartile range ($\Phi_{\delta h_i}$). For each constructed stratigraphic column we tracked the interquartile range of the distribution of elevation increments, the mean of the elevation increments $\langle \delta h_i \rangle$, and the estimated mean of the preserved bed thicknesses, $\langle D_{st} \rangle$, which fully characterizes the distribution of bed thicknesses since they are well described by an exponential distribution.

[33] Figure 11a shows how the non-dimensional bed thickness (calculated by taking the ratio of the estimated mean bed thickness to the background net depositional rate, $\langle D_{st} \rangle / \langle \delta h_i \rangle$) varies as a function of the non-dimensional interquartile range of the distribution of elevation increments ($\Phi_{\delta h_i}$) for synthetic stratigraphic columns created by both thin-tailed (exponential) and heavy-tailed (power law) elevation increment distributions. Note that since both axes of Figure 11a are non-dimensional, one can compare systems of different absolute scale, but similar in their ratio of surface variability to mean background deposition rate. Each data point on Figure 11 represents the outcome of a single 1D stochastic model of sedimentation as outlined in section 4. Utilizing symmetrical distributions and user specified values of the non-dimensional interquartile range of the distribution

of elevation increments, we constructed the preserved bed thickness distributions from which we estimated the mean preserved bed thickness, $\langle D_{st} \rangle$. For time series constructed with up to 100,000 increments (the maximum time series length generated in this analysis) we noted no difference in the shape of the relationship between the non-dimensional bed thickness and the non-dimensional interquartile range of the distribution of elevation increments. Interestingly, we found that the data from the DB-03 experiment nicely plot on the curve computed from the 1D stochastic models. As the coefficient of variation (CV) is a more commonly used metric to compare a distribution's variability to its mean we also present a plot of the non-dimensional bed thickness versus the coefficient of variation of the surface elevation increments, while acknowledging that the coefficient of variation would not formally exist for heavy-tailed distribution of elevation increments (Figure 11b).

[34] As the non-dimensional interquartile range of the distribution of elevation increments increases from a minimum possible value of zero, the non-dimensional bed thickness decreases until it reaches a global minimum of approximately 7 at a value of $\Phi_{\delta h_i} \sim 1.4$. Further increases in the non-dimensional interquartile range of the distribution of elevation increments result in an increase of the non-dimensional bed thickness with the rate of increase characterized by a slope equal to ~ 1.4. In summary, Figure 11 illustrates that a large value for the mean of a bed thickness distribution relative to the background deposition rate can result from either extremely low or extremely high variability in elevation increments relative to the background drift. On the left-hand side of this relationship in Figure 11 ($\Phi_{\delta h_i} < 1.4$), increasing the variability of elevation increments, for a given background drift, decreases the mean bed thickness in the resulting stratigraphic column. On this side of the plot the variability of elevation increments is small relative to the mean background drift, thus erosional events are rare and the stratigraphic column is constructed from a broad distribution of thick deposits. In other words, increasing the surface variability tends to break thick deposits into smaller units reducing thus the mean of the preserved bed thicknesses. On the right-hand side of this relationship in Figure 11 ($\Phi_{\delta h_i} > 1.4$) increasing the variability of elevation increments, for a given background drift, increases the mean bed thickness in the resulting stratigraphic column. On this side of the plot the variability of elevation increments is large relative to the mean, thus most
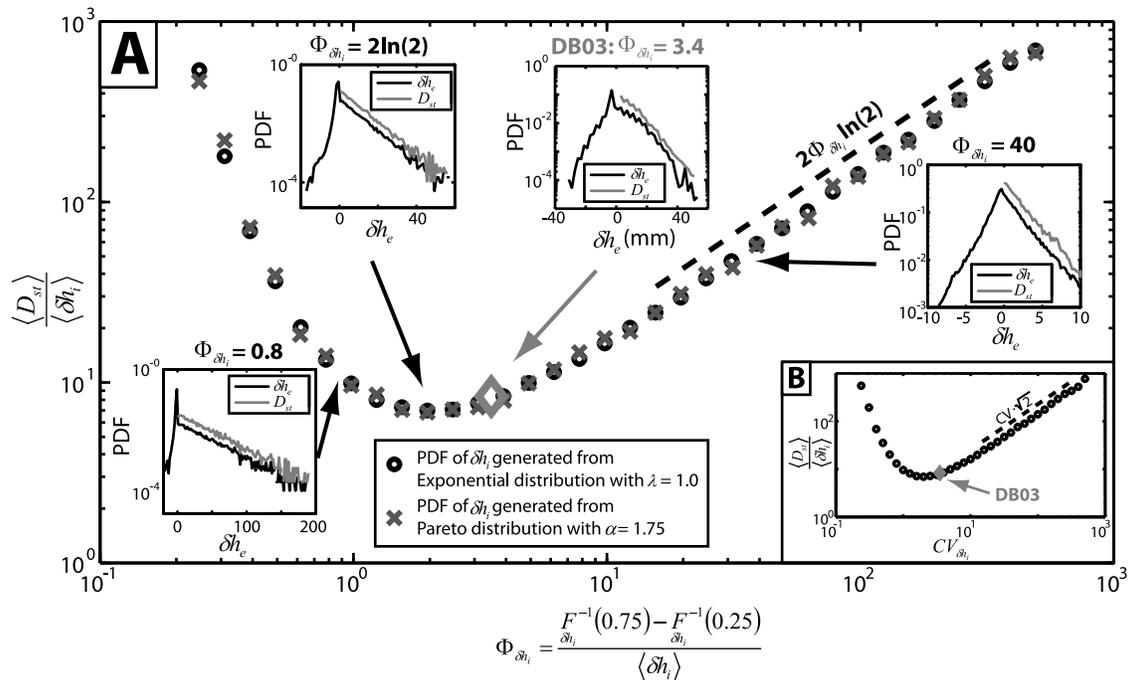
Figure 11. Model results documenting relationship between (a) $\Phi_{\delta h_i}$ and (b) $CV_{\delta h_i}$ for surface elevation fluctuations and $\frac{\langle D_{st} \rangle}{\langle \delta h_i \rangle}$ generated from 1D synthetic stratigraphy models with input PDF of $\delta h_i(t)$ generated from exponential distribution with $\lambda = 1.0$ are shown with black open circles, while 1D models with input PDF of $\delta h_i(t)$ generated from Pareto distribution with $\alpha = 1.75$ are shown with gray crosses. Gray open triangle indicates relationship between data from DB-03 experiment. Insert plots illustrate shape of Kolmogorov increments, $\delta h_e(t)$, and resulting bed thickness, D_{st}^e, distributions for 1D models with 3 $\Phi_{\delta h_i}$ values. Distributions displayed in insert plots resulted from elevation increments, $\delta h_i(t)$ generated from Pareto distributions with $\alpha = 1.75$.

sediment that is deposited is eventually removed by future erosional events and the stratigraphic column is constructed from sediment that is reworked by a broad distribution of erosional events.

[35] Analysis of the Kolmogorov event, $\delta h_e(t)$, distributions provides additional insight into the processes responsible for the shape of the relationship between the non-dimensional interquartile range of the distribution of elevation increments and the non-dimensional bed thickness. All model runs for Figure 11 had symmetrical distributions of elevation increments. Insert plots within Figure 11 define the shape of the Kolmogorov event's distributions for three values of the non-dimensional interquartile range of the distribution of elevation increments. For conditions where $\Phi_{\delta h_i} > 1.4$ the resulting distribution of Kolmogorov events is approximately symmetrical in form. As the value of non-dimensional interquartile range of the distribution of elevation increments, $\Phi_{\delta h_i}$, decreases below a value of 1.4, the distribution of the Kolmogorov events becomes increasingly asymmetric with more weight on the positive (D_e) side of the distribution than the negative end (E_e) of the distribution.

[36] For all conditions analyzed, the mapping of elevation increments to Kolmogorov events is associated with a significant thinning of the tail of the distribution. This results in depositional and erosional events (D_e and E_e) that are well described by thin-tailed, exponential distributions. This allows us to compare the estimated scale parameters of the depositional and erosional events, $\hat{\mu}_{D_e}$ and $\hat{\mu}_{E_e}$, respectively.

For conditions where $\Phi_{\delta h_i} < 1.4$, we find that the estimated mean of the depositional events is much larger than the estimated mean of the erosional events ($\hat{\mu}_{D_e} \gg \hat{\mu}_{E_e}$) and thus the distribution of the Kolmogorov events is asymmetric. However, as the value of the non-dimensional interquartile range of the distribution of elevation increments increases, the difference between the estimated means of the depositional and erosional events decreases and as a result the mean of the preserved bed thicknesses ($\hat{\mu}_{D_{st}}$) decreases. This is summarized in the following scaling relationship:

$$\hat{\mu}_{D_{st}} \sim \hat{\mu}_{D_e} - \hat{\mu}_{E_e} \qquad (12)$$

The decrease in the estimated mean of the preserved bed thicknesses continues until the distributions of the depositional and erosional events are roughly symmetrical. At this location, the $\delta h_e(t)$ distribution can be approximated as a Laplace distribution. We note that the interquartile range of a Laplace distribution (see equation (7)) is equal to $2b \ln(2)$ or approximately $1.4b$, where b is the scale parameter of the Laplace distribution. We observe that the global minimum in the values of non-dimensional bed thickness occurs at a value where the background net depositional rate ($\langle \delta h_i \rangle$) is equal to the scale parameter (b) of the best fit Laplace distribution of the Kolmogorov events suggesting that the filtering of information contained within the tails of an elevation increments distribution also strongly influences the relationship shown in Figure 11. Above the value of $\Phi_{\delta h_i}$

~1.4 the Kolmogorov events' distribution is well described by a Laplace distribution (i.e., symmetrical distribution of depositional and erosional events), and increasing the value of the non-dimensional interquartile range of the distribution of elevation increments results in an increase of the non-dimensional bed thickness at a rate characterized by a slope approximately equal to 1.4 (or approximately equal to 2ln (2)). In essence, for symmetrical elevation events, an increase in the variability of elevation events always causes an increase in the mean bed thickness, similar to the finding by *Paola and Borgman* [1991].

[37] Finally, to test the sampling interval scale-dependence of the trend observed in Figure 11, we generated elevation time series as discussed above and calculated the non-dimensional interquartile range of the distribution of the elevation increments and the non-dimensional bed thickness at the finest resolution. We then subsampled the elevation time series, extracting every nth elevation measurement, and recalculated the non-dimensional interquartile range of the distribution of the elevation increments and the non-dimensional bed thickness of the new subsampled elevation time series. We find that the non-dimensional interquartile range of the distribution of the elevation increments and the non-dimensional bed thickness from the subsampled elevation time series plots on the trend that was generated from the elevation time series considered at the finest resolution. In other words, we find that the relationship established in Figure 11 is robust to changes in scales of measurement of the surface elevation increments.

5.3. Implications for Stratigraphy

[38] Analysis of the DB-03 experimental data and the 1D stochastic models that generated synthetic stratigraphy suggests a predictable relationship between the variability in topography and the mean bed thickness of a stratigraphic column. Environments with near-symmetric distributions of elevation increments (both thin- and heavy-tailed), and near-symmetric distributions of periods of depositional and erosional events produce stratigraphic columns composed of exponentially distributed beds. The fact that most reported unconformity-bounded bed thickness distributions are exponential suggests that field scale distributions of elevation increments and periods of depositional and erosional events are in fact often symmetrical. While yet untested, the relationship presented in Figure 11 might also aid in the analysis and identification of paleo-environments. For example, suppose for the sake of argument that, for a given background deposition rate the appropriately scaled variability in surface evolution of braided rivers were greater than in meandering rivers. Then the preserved bed thickness distributions generated from braided rivers would plot more toward the right-hand side of Figure 11 compared to bed distributions resulting from meandering rivers. We believe these questions pose an interesting line of investigation for future experimental studies. Further questions which remain to be addressed include 1) the relationship between the Kolmogorov definition of beds, defined as strata deposited between successive preserved erosional surfaces, and beds defined in outcrops as strata bounded above and below by distinct textural horizons. This might be achieved in controlled laboratory experiments where time series of elevation can be compared to spatially referenced images of preserved

physical stratigraphy. 2) What is the relationship between surface variability and resulting bed-thickness statistics for systems with nested distributions of surface topography. For instance, how do the PDFs of topographic fluctuations relate to bed thicknesses in avulsive river systems with river channel bottoms covered by depth-limited dunes?

[39] Finally, in our previous study on the statistics of surface dynamics in depositional braided fluvial systems, *Ganti et al.* [2011] found that several distributions associated with surface dynamics follow truncated Pareto distributions. They reported that the truncation scales for these distributions are set by the depths of channels constructing a package of sediment and the time scale of avulsion associated with these channels. This finding also has implications for the conversion of elevation increments to stratigraphic beds thickness. The truncation at a scale associated with the roughness of the surface topography essentially makes the tails of the distribution of elevation increments thinner than the case where the distribution is not truncated. As a result, the distributions of the Kolmogorov events and the preserved bed thickness that result from a truncated parent distribution will have tails that exhibit faster decay (lesser weight in extremes) than distributions arising from non-truncated parent distributions, adding to the prevalence of exponential-like bed thickness distributions in the stratigraphic record.

[40] All in all, then, we see two broad categories of bed creation in the stratigraphic record. The first, which we believe is the most common, involves reworking of the surface by a combination of upward and downward increments (deposition and erosion, or "cut-and-fill"). We have shown here that this case is expected to produce exponential-type (thin-tailed) bed thickness distributions regardless of whether the distributions of the associated sediment surface dynamics are thin- or heavy-tailed. The second case is that in which there is strong asymmetry between deposition and erosion. This could mean that the depositional events are heavy-tailed and the erosional events thin-tailed, for which we are not aware of any field examples; or more simply that the erosional events are absent or negligible, for example at the distal end of the depositional system. With no erosional modification, the beds are then a faithful record of the events that produced them. This is the case studied, for example, by *Rothman et al.* [1994], and here if the events have a heavy-tailed distribution then so will the deposits.

6. Conclusions

[41] Following a previous study by the authors [*Ganti et al.*, 2011], this paper presents an extensive analysis of experimental and stochastically generated surface morphology to quantitatively examine the relation between surface elevation evolution and the resulting stratigraphy. The main results are summarized as follows:

[42] 1. Thin-tailed (e.g., exponential) bed thickness distributions result from heavy-tailed surface evolution statistics, as evidenced from both the laboratory experimental data and numerical simulations. We showed that this thinning of the tail of the distribution occurs in environments where the distributions of the surface elevation increments and periods of depositional and erosional events (t_d and t_e) have positive means and are symmetric in shape.

[43] 2. Asymmetry in parent topographic PDFs results in bed thickness distributions that carry some of the heavy-tailed statistics present in their parent distributions. Truncation of the parent distribution tails due to depositional processes further reduces the chance of occurrence of extremes in preserved bed thicknesses compared to their parent distributions. The implication of this result adds to the prevalence of exponential bed thicknesses as heavy-tailed distributions in nature are often truncated at some scale.

[44] 3. The interquartile range (difference between the 75th and 25th quartiles) of the surface elevation increments can serve as a predictor of mean bed thickness of the stratigraphic deposit. This relationship holds for both thin and heavy-tailed surface statistics and demonstrates that information related to the variability of surface fluctuations is stored in the stratigraphic record.

Notation

b scale parameter of Laplace distribution.
CV coefficient of variation.
$CV_{\delta h_i}$ coefficient of variation of elevation increments.
D_e magnitude of depositional events.
D_i positive elevation increments, $\delta h(t) > 0$.
D_{st} thickness of stratigraphic deposits.
D_{st}^e thickness of stratigraphic deposits constructed from elevation time series.
$\hat{D}_{st}^e$ estimated thickness of stratigraphic deposits from summation of consecutive depositional and erosional events.
D_{st}^s thickness of stratigraphic deposits measured from physical stratigraphy.
E_e magnitude of erosional events.
E_i negative elevation increments, $\delta h(t) < 0$.
$h(t)$ elevation time series of experimental data.
IQR Interquartile range.
K_c Kolmogorov coefficient.
t time.
t_d durations of depositional events.
t_e durations of erosional events.
t_{st} time interval demarcating the boundaries of the deposit D_{st}.
$\hat{\alpha}_1$ tail index of truncated Pareto distribution for D_i.
$\hat{\alpha}_2$ tail index of truncated Pareto distribution for E_i.
$\hat{\alpha}'_1$ tail index of truncated Pareto distribution for D_e.
$\hat{\alpha}'_2$ tail index of truncated Pareto distribution for E_e.
$\delta h_i(t)$ elevation increments in time.
$\delta h_e(t)$ Kolmogorov events.
Φ Nondimensional interquartile range.
$\Phi_{\delta h_i}$ Nondimensional interquartile range of elevation increments.
γ lower bound of truncated Pareto distribution.
λ rate parameter of Exponential distribution.
$\hat{\lambda}_{t_d}$ rate parameter of fitted Exponential distribution to t_d.
$\hat{\lambda}_{t_e}$ rate parameter of fitted Exponential distribution to t_e.
μ mean of Laplace distribution and double Pareto distribution.
$\hat{\mu}_{D_e}$ scale parameter of fitted exponential distribution to D_e.
$\hat{\mu}_{D_{st}}$ scale parameter of fitted exponential distribution to D_{st}.
$\hat{\mu}_{E_e}$ scale parameter of fitted exponential distribution to E_e.
σ standard deviation of elevation increments.
ν upper bound of truncated Pareto distribution.

References

Ager, D. V. (1993), *The Nature of the Stratigraphic Record*, 151 pp., John Wiley, New York.

Bailey, R. J., and D. G. Smith (2010), Scaling in stratigraphic data series: Implications for practical stratigraphy, *First Break*, *28*, 57–66.

Beeden, R. D. (1983), Sedimentology of some turbidites and related rocks from the Cloridorme Group, Ordovician, Quebec, MS thesis, 254 pp., McMaster Univ., Hamilton, Ontario, Canada.

Carlson, J., and J. P. Grotzinger (2001), Submarine fan environment inferred from turbidite thickness distributions, *Sedimentology*, *48*(6), 1331–1351, doi:10.1046/j.1365-3091.2001.00426.x.

Dacey, M. F. (1979), Models of bed formation, *J. Int. Assoc. Math. Geol.*, *11*(6), 655–668, doi:10.1007/BF01031890.

Drummond, C. N., and P. J. Dugan (1999), Self-organizing models of shallow-water carbonate accumulation, *J. Sediment. Res.*, *69*(4), 939–946.

Drummond, C. N., and B. H. Wilkinson (1996), Stratal thickness frequencies and the prevalence of orderedness in stratigraphic sequences, *J. Geol.*, *104*, 1–18, doi:10.1086/629798.

Endo, N. (2010), Inverse problem and solution of the Kolmogorov model for bed thickness distribution, *Math. Geosci.*, *42*(8), 955–968, doi:10.1007/s11004-010-9300-y.

Foufoula-Georgiou, E., V. Ganti, and W. E. Dietrich (2010), A nonlocal theory of sediment transport on hillslopes, *J. Geophys. Res.*, *115*, F00A16, doi:10.1029/2009JF001280.

Ganti, V., M. M. Meerschaert, E. Foufoula-Georgiou, E. Viparelli, and G. Parker (2010), Normal and anomalous diffusion of gravel tracer particles in rivers, *J. Geophys. Res.*, *115*, F00A12, doi:10.1029/2008JF001222.

Ganti, V., K. M. Straub, E. Foufoula-Georgiou, and C. Paola (2011), Space-time dynamics of depositional systems: Experimental evidence and theoretical modeling of heavy-tailed statistics, *J. Geophys. Res.*, *116*, F02011, doi:10.1029/2010JF001893.

Gardner, T. W., D. W. Jorgensen, C. Shuan, and C. R. Lemieux (1987), Geomorphic and tectonic process rates: Effects of measured time interval, *Geology*, *15*, 259–261, doi:10.1130/0091-7613(1987)15<259:GATPRE>2.0.CO;2.

Hajek, E. A., P. L. Heller, and B. A. Sheets (2010), Significance of channel-belt clustering in alluvial basins, *Geology*, *38*(6), 535–538, doi:10.1130/G30783.1.

Jerolmack, D. J., and D. Mohrig (2005), Frozen dynamics of migrating bedforms, *Geology*, *33*(1), 57–60, doi:10.1130/G20897.1.

Jerolmack, D. J., and P. Sadler (2007), Transience and persistence in the depositional record of continental margins, *J. Geophys. Res.*, *112*, F03S13, doi:10.1029/2006JF000555.

Kolmogorov, A. N. (1951), *Solution of a Problem in Probability Theory Connected With the Problem of the Mechanism of Stratification*, Am. Math. Soc., New York.

Leclair, S. F., and J. S. Bridge (2001), Quantitative interpretation of sedimentary structures formed by river dunes, *J. Sediment. Res.*, *71*(5), 713–716, doi:10.1306/2DC40962-0E47-11D7-8643000102C1865D.

Martin, J. M. (2007), Quantitative sequence stratigraphy, PhD thesis, 204 pp., Univ. of Minn., Minneapolis.

Mizutani, S., and I. Hattori (1972), Stochastic analysis of bed-thickness distribution of sediments, *Math. Geol.*, *4*, 123–146, doi:10.1007/BF02080298.

Molchan, G. M., and D. L. Turcotte (2002), A stochastic model of sedimentation: Probabilities and multifractality, *Eur. J. Appl. Math.*, *13*, 371–383, doi:10.1017/S0956792502004850.

Muto, T. (1995), The Kolmogorov model of bed-thickness distribution: An assessment based on numerical simulation and field-data analysis, *Terra Nova*, 7, 417–423, doi:10.1111/j.1365-3121.1995.tb00537.x.

Paola, C. (2000), Quantitative models of sedimentary basin filling, *Sedimentology*, 47, 121–178, doi:10.1046/j.1365-3091.2000.00006.x.

Paola, C., and L. Borgman (1991), Reconstructing random topography from preserved stratification, *Sedimentology*, 38, 553–565, doi:10.1111/j.1365-3091.1991.tb01008.x.

Paola, C., K. Straub, D. Mohrig, and L. Reinhardt (2009), The "unreasonable effectiveness" of stratigraphic and geomorphic experiments, *Earth Sci. Rev.*, 97, 1–43, doi:10.1016/j.earscirev.2009.05.003.

Pelletier, J. D., and D. L. Turcotte (1997), Sythetic stratigraphy with a stochastic diffusion model of fluvial sedimentation, *J. Sediment. Res.*, 67, 1060–1067.

Pirmez, C., R. N. Hiscott, and J. D. Kronen (1997), Sandy turbidite successions at the base of channel-levee systems of the Amazon fan revealed by FMS logs and cores: Unraveling the facies architecture of large submarine fans, in *Proceedings of the Ocean Drilling Program, Scientific Results*, edited by R. D. Flood et al., pp. 7–33, Ocean Drill. Prog., College Station, Tex.

Rothman, D. H., J. P. Grotzinger, and P. Flemings (1994), Scaling in turbidite deposition, *J. Sediment. Res.*, 64(1), 59–67.

Sadler, P. M. (1981), Sediment accumulation rates and the completeness of stratigraphic sections, *J. Geol.*, 89, 569–584, doi:10.1086/628623.

Schumer, R., and D. J. Jerolmack (2009), Real and apparent changes in sediment deposition rates through time, *J. Geophys. Res.*, 114, F00A06, doi:10.1029/2009JF001266.

Schwarzacher, W. (1975), *Sedimentation Models and Quantitative Stratigraphy*, 382 pp., Elsevier, Amsterdam.

Sheets, B. A., T. A. Hickson, and C. Paola (2002), Assembling the stratigraphic record: Depositional patterns and time-scales in an experimental alluvial basin, *Basin Res.*, 14, 287–301, doi:10.1046/j.1365-2117.2002.00185.x.

Sheets, B. A., C. Paola, and J. M. Kelberer (2007), Creation and preservation of channel-form sand bodies in an experimental alluvial system, in *Sedimentary Processes, Environments and Basins*, edited by G. Nichols, E. Williams, and C. Paola, pp. 555–567, Blackwell, Oxford, U. K., doi:10.1002/9781444304411.ch22

Sinclair, H. D., and P. A. Cowie (2003), Basin-floor topography and the scaling of turbidites, *J. Geol.*, 111, 277–299, doi:10.1086/373969.

Stark, C. P., E. Foufoula-Georgiou, and V. Ganti (2009), A nonlocal theory of sediment buffering and bedrock channel evolution, *J. Geophys. Res.*, 114, F01029, doi:10.1029/2008JF000981.

Straub, K. M., C. Paola, D. Mohrig, M. A. Wolinsky, and T. George (2009), Compensational stacking of channelized sedimentary deposits, *J. Sediment. Res.*, 79(9), 673–688, doi:10.2110/jsr.2009.070.

Strauss, D., and P. M. Sadler (1989), Stochastic-Models for the Completeness of Stratigraphic Sections, *Math. Geol.*, 21(1), 37–59, doi:10.1007/BF00897239.

Strong, N., and C. Paola (2008), Valleys that never were: Time surfaces versus stratigraphic surfaces, *J. Sediment. Res.*, 78(8), 579–593, doi:10.2110/jsr.2008.059.

Sylvester, Z. (2007), Turbidite bed thickness distributions: Methods and pitfalls of analysis and modelling, *Sedimentology*, 54, 847–870, doi:10.1111/j.1365-3091.2007.00863.x.

Talling, P. J. (2001), On the frequency distribution of turbidite thicknesses, *Sedimentology*, 48, 1297–1329, doi:10.1046/j.1365-3091.2001.00423.x.

Tipper, J. C. (1983), Rates of sedimentation, and stratigraphical completeness, *Nature*, 302(5910), 696–698, doi:10.1038/302696a0.

E. Foufoula-Georgiou and V. Ganti, St. Anthony Falls Laboratory, Department of Civil Engineering, University of Minnesota, Minneapolis, MN 55414, USA.

C. Paola, St. Anthony Falls Laboratory, Department of Geology and Geophysics, University of Minnesota, Minneapolis, MN 55414, USA.

K. M. Straub, Department of Earth and Environmental Sciences, Tulane University, New Orleans, LA 70118, USA. (kmstraub@tulane.edu)